Flow behavior at different shear rates for dry powders

A. Singh and S. Luding
Multi Scale Mechanics, University of Twente, Enschede, The Netherlands
Email: a.singh@ctw.utwente.nl

ABSTRACT
Using Discrete Element Simulations (DEM), an effort is made to study the so called "Split bottom ring shear cell" where a slow, quasi-static deformation leads to wide shear bands. Density, velocity and deformation gradients as well as structure and stress tensors, can be computed by a single simulation, by applying time and (local) space averaging. Here, we focus on different shear rates by increasing the rate of rotation of the system.

INTRODUCTION
Granular matter plays an important role in our everyday life and therefore receives a growing interest in physics and engineering. Many open questions exist about the flow of such matter. The intrinsically nonlinear and dissipative nature of the interactions between the particles leads to a great deal of interesting phenomena like segregation, jamming, clustering, and shear-band formation.
Discrete Element Methods (DEM) allow for the specification of particle properties and interaction laws and then the numerical solution of Newton's equations of motion [1,2]. One goal is to derive macroscopic continuum constitutive relations and their relevant parameters (based on particle and contact properties) from experimental and numerical tests on representative samples. This means to bridge the gap between the microscopic properties and the macroscopic mechanical behavior. Methods and tools for this so called micro-macro transition are often applied on small so-called representative volume elements (RVE) [3-8].
In this study, both local space-averaging as well as time-averaging is applied for a (presumed) steady state in the case of a ring-shear cell with split bottom, as recently presented [9,10]. Constitutive relations involving a range of densities, pressures and shear-rates can thus be obtained from a single simulation. In this study, the focus is on different shear rates. In this study, the system is randomly agitated by shearing faster and faster. Other means of random agitation, like Brownian white noise, will be studied elsewhere.

SPLIT-BOTTOM RING SHEAR CELL
In the split-bottom ring shear cell [9,10], the shear band is initiated from the bottom split, far away from the side walls. The velocity field is well approximated by an error function, see Refs. [9-12], where it was observed that the center of the shearband is moving inwards while the width is increasing from bottom to top.
Since the geometry is axisymmetric, to save the computing time, only a quarter of the ring-shaped geometry is simulated, using quarter periodic boundary conditions in angular direction. (In top-view, see [8,13], when a particle leaves the quarter system downwards it enters at the same radial position from the right – with according, unchanged velocity in cylindrical coordinates). The walls are cylindrical and are roughened due to some (about 3 per-cent of the total number) attached particles [8,11,13]. The outer cylinder wall, with radius R_o = 0.110 m, and part of the bottom $r > R_S$ = 0.085 m, are rotating around the symmetry axis with the same rotation rate f, while the inner wall at radius R_i = 0.0147 m, and the attached bottom-disk $r < R_S$ remain at rest. First, the simulation runs for more than 50 s with a rotation rate of, for example, f_o = 0.01 s^{-1}, of the outer cylinder [9,10], with angular velocity $\Omega = 2\pi f_o$. In the following different rotation rates f will be compared. For the average, only large times are taken into account, thus disregarding the transient behavior at the onset of shear.

Translational invariance is assumed in the tangential ϕ -direction, and averaging is thus performed over toroidal volumes and over many snapshots in time (typically 40-60), leading to fields $Q(r,z)$ as function of the radial and vertical positions. Here, averaging is performed with spacings $\Delta r \approx 0.0025$ m and $\Delta z \approx 0.0012$ m in radial and vertical direction. The choice of the spacing is arbitrary, since it does not affect the results discussed below if varied somewhat. However, much smaller spacing leads to bad statistics and stronger fluctuations, while much larger spacing leads to poor resolution and thus loss of information.
From the velocity gradient, the strain rate is obtained [8,13] as

$$\dot{\gamma} = \frac{1}{2}\sqrt{\left(\frac{\partial v_\varphi}{\partial r} - \frac{v_\varphi}{r}\right)^2 + \left(\frac{\partial v_\varphi}{\partial z}\right)^2} \qquad (1)$$

where the geometrical term, v_φ / r comes from the cylindrical coordinate system. From the simulations, one can determine the stress tensor

$$\sigma_{\alpha\beta} = \frac{1}{V}\left(\sum_i m_i v_i^\alpha \otimes v_i^\beta - \sum_{c\in V} f_c^\alpha l_c^\beta\right) \qquad (2)$$

with the forces f_c and branch vectors l_c components. The sum includes the kinetic energy of the particles and the contact-force dyadic product with the branch vector, in the vicinity of the averaging volume, V, weighted according to their vicinity. Since the σ_{rz} component is small compared to other averaged non-diagonal stress terms, the shear stress can be defined in analogy to the velocity gradient [8,13]:

$$|\tau| = \sqrt{\sigma_{r\phi}^2 + \sigma_{z\phi}^2} \qquad (3)$$

In the following, we present a detailed study of the shear cell for different rotation rates of the bottom (f = 0.005 sec^{-1}, 0.01 sec^{-1}, 0.02 sec^{-1} and 0.04 sec^{-1}).

RESULTS

From DEM simulations, coordination number and energy can be obtained as function of time. In Fig.1 (Left) we plot the average number of (contacts-6) for different rotation rates, where the value 6, i.e. the isostatic coordination number in 3D, for frictionless particles, is subtracted in order to see the difference from the isostatic situation. The strain rates increase with the rotation rate of the bottom and the higher the strain rate the smaller is the number of contacts, partly due to dilatancy and partly due to an increased kinetic energy.
When the total kinetic energy of the system (excluding potential energy due to gravity, but including the contact elastic potential energy) is plotted against scaled time t^* (scaled with relative rotation rate $t^* = t\, f / f_o$), see Fig. 1 (Right), a beautiful scaling is observed (note that all energy data fall on the top of each other). By scaling time with the rotation rate, we are rotating the system by same amount per scaled time-unit, and hence do the same work, irrespective of rotation rate. The fact that the highest rotation rate is slightly off indicates, that for $f > 0.04$, the quasi-static regime is left and the system enters the dynamic regime.
The stress tensor can be calculated from a single DEM simulation, see Eq. (2) above, for various pressures and shear rates. In Fig. 2, the shear stress $|\tau|$, see Eq. (3) above, and shear stress intensity $|\tau| / p$ are plotted against the pressure $p = \mathrm{tr}(\sigma)/3$, for local scaled strain rates $\gamma^* = \dot{\gamma}\, f / f_o$ greater than 0.08 (scaled with rotation speed of the base).

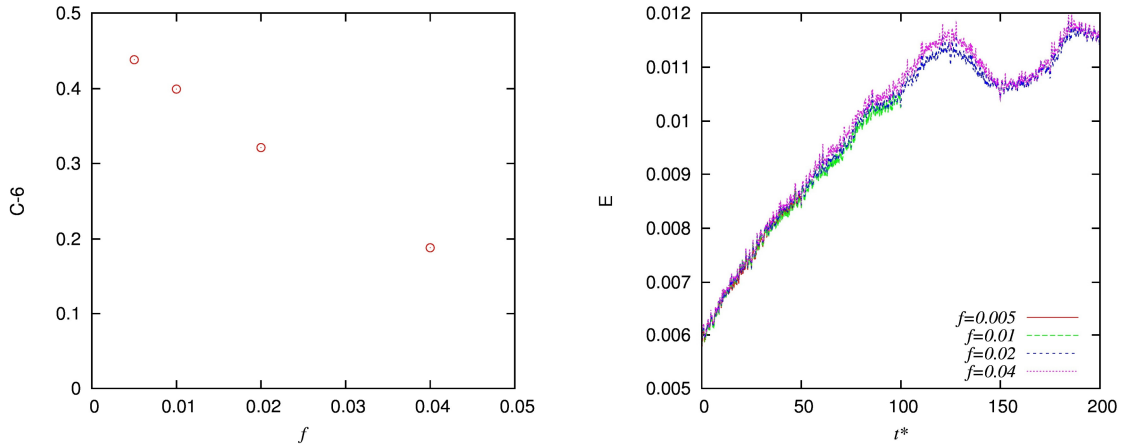

Fig. 1.(Left) Average number of contacts per particle that is larger than six, *C*-6, plotted against rotation rate *f*. (Right) Total Energy plotted against scaled time *t**.

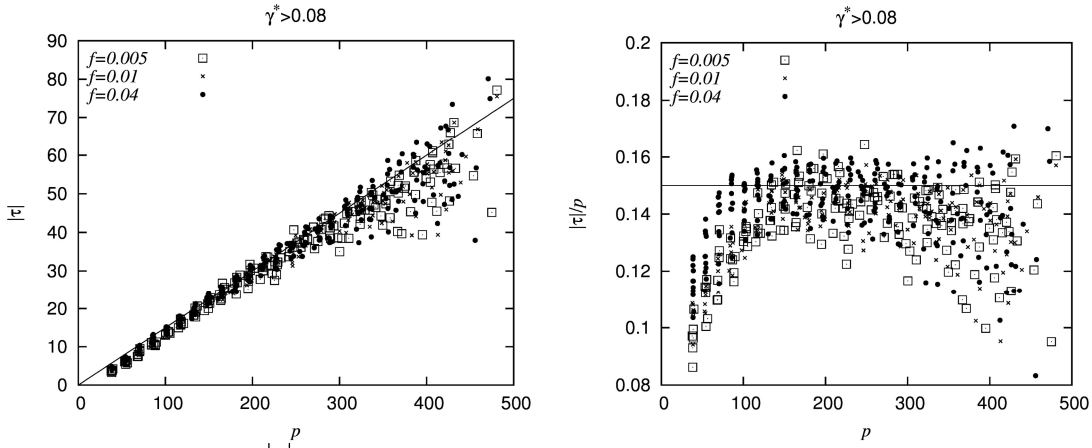

Fig. 2. (Left) Shear Stress $|\tau|$ plotted against pressure p, for scaled shear rates γ*>0.08, the different symbols correspond to different rotation rates as given in the inset. (Right) Shear stress intensity $|\tau|/p$, plotted against pressure p for the same data as left.

As can be seen from Fig. 2, the data for different rotation rates coincide for small rotation rates and smaller pressure, but somewhat deviate for the higher rotation rate and higher pressure. From the shear stress and (almost) constant shear stress intensity in the shear zone, one can determine the Mohr-Coulomb-type friction angle of the equivalent macroscopic constitutive law, which is identical to the one from previous simulations with frictionless materials [8]. In Fig. 2 (right), we see that there is a weak systematic variation of $|\tau|/p$ with pressure: an increase up to p =200 Nm^{-2} and a weak decrease for higher p, together with stronger fluctuations. We attribute the deviation for large pressure to the effect of different rates of rotation. The local shear rate will be increased more prominently at the bottom (as particles which are closer to bottom will sense the effect of the increased rotation rate at the split more directly than particles at the top).

CONCLUSIONS

Simulations of a split-bottom Couette ring shear cell show perfect qualitative and good quantitative agreement with experiments [8,12,13]. Different rates of rotation of the bottom were used to agitate the system and thus to insert more and more energy. Scaling could be achieved

for the total energy and Mohr-Coulomb-type yield locus plots, where the highest shear-rate was at the edge of the quasi-static regime, showing first signs of dynamic effects.
A more detailed analysis for shear stress, structure, fluctuation kinetic energy (granular temperature), as well as a detailed eigenvalue analysis is still to be done to understand the effect of driving, i.e., energy input, on the constitutive flow behavior of particle systems.

ACKNOWLEDGEMENTS

We acknowledge support from the research program of the Stichting voor Fundamenteel Onderzoek der Materie (FOM), which is financially supported by the "Nederlandse Organisatie voor Wetenschappelijk Onderzoek" (NWO), (project number: 07CJR06).

REFRENCES

[1] M. P. Allen and D. J. Tildesley. Computer Simulation of Liquids. Oxford University Press, Oxford, 1987.
[2] P. A. Cundall. A computer model for simulating progressive, large-scale movements in blocky rock systems. In The International Symposium on rock mechanics, Nancy, France, 1971.
[3] F. Alonso-Marroquin and H.J. Herrmann. Investigation of the incremental response of soils using a discrete element model. J. of Eng. Math., 52:11–34, 2005.
[4] K. Bagi. Microstructural stress tensor of granular assemblies with volume forces. J. Appl. Mech., 66:934–936, 1999.
[5] P. A. Vermeer, S. Diebels, W. Ehlers, H. J. Herrmann, S. Luding, and E. Ramm, editors. Continuous and Discontinuous Modelling of Cohesive Frictional Materials, Berlin, 2001. Springer. Lecture Notes in Physics 568.
[6] M. Lätzel, S. Luding, and H. J. Herrmann. Macroscopic material properties from quasistatic, microscopic simulations of a two-dimensional shear-cell. Granular Matter, 2(3):123–135, 2000.
[7] S. Luding. Cohesive frictional powders: Contact models for tension. Granular Matter, 10:235–246, 2008.
[8] S. Luding. The effect of friction on wide shear bands. Particulate Science and Technology, 26(1):33–42, 2008.
[9] D. Fenistein, J. W. van de Meent, and M. van Hecke. Universal and wide shear zones in granular bulk flow. Phys. Rev. Lett., 92:094301, 2004
[10] D. Fenistein and M. van Hecke. Kinematics – wide shear zones in granular bulk flow. Nature, 425(6955):256, 2003.
[11] S. Luding. Particulate solids modeling with discrete element methods. In P. Massaci, G. Bonifazi, and S. Serranti, editors, CHoPS-05 CD Proceedings, pages 1–10, Tel Aviv, 2006. ORTRA.
[12] S. Luding. Micro-macro transition for anisotropic, frictional granular packings. Int. J. Sol. Struct., 41:5821–5836, 2004.
[13] S. Luding. Constitutive relations for the shear band evolution in granular matter under large strain. Particuology, 6(6):501–505, 2008.
[14] M. Depken, W. van Saarloos, and M. van Hecke. Continuum approach to wide shear zones in quasistatic granular matter. Phys. Rev. E, 73:031302, 2006.